Probing structural inhomogeneity of graphene layers via nonlinear optical scattering

Anton Y. Bykov,[1,*] Pavel S. Rusakov,[2] Elena D. Obraztsova,[2] and Tatiana V. Murzina[1]

[1]*Department of Physics, Moscow State University, 119991 Moscow, Russia*

[2]*A.M. Prokhorov General Physics Institute, RAS, 38 Vavilov Street, 119991 Moscow, Russia*

*Corresponding author: lancaster@shg.ru

Incoherent optical second harmonic generation (SHG) is studied from series of multilayer graphene samples of various thickness manufactured by chemical vapor deposition technique and deposited over 150 µm thick glass slides. Two different values of the correlation lengths are obtained from the linear and SHG indicatrices and reveal the existence of two types of optical scatterers. The first one is associated with homogeneous graphene areas, while the second one originates from wrinkles at the interdomain boundaries. Second harmonic imaging microscopy used to map the distribution of the second-order polarization at the nanoscale confirms the results of the nonlinear scattering data. © 2013 Optical Society of America

OCIS codes: (160.4236) Nanomaterials; (190.4350) Nonlinear optics at surfaces; (120.5820) Scattering measurements; (180.4315) Nonlinear microscopy.

http://dx.doi.org/10.1364/OL.38.004589

Graphene that is a plain two-dimensional allotrope of carbon has attracted substantial interest over recent years due to its unique electronic, thermal, mechanical, and optical properties [1,2], as well as because of high inherent potential for future applications as field-effect transistors [3] and conductive coatings [4]. In the meantime, most of the graphene research was focused entirely on monolayers because of their unconventional band structure [5]. However, in crystalline multilayers, graphene still offers a number of promising electronic and optical properties including a universal fine structure constant-defined absorption over the visible and near infrared wavelength range [6], Raman scattering in graphene [7,8], hot-carrier photoluminescence [9], and terahertz plasmonics [10]. Even the band structure of a monolayer can be preserved due to effective decoupling of adjacent layers for the multilayer films with a twist [11–13]. Moreover, crystalline graphene films are the ones that are produced in all currently available scalable graphene production techniques such as chemical vapor deposition (CVD) [4,14,15] or thermal decomposition of silicon carbide [12]. Therefore, their investigation by the methods other than conventional electron microscopy is in high demand.

Recently, a number of studies regarding the nonlinear-optical response of graphene has been reported. Second harmonic generation (SHG), studied both theoretically [16,17] and experimentally [18], showed that the intrinsic second-order nonlinearity of graphene, especially in crystalline films, is rather weak unless enhanced by some kind of resonance or external symmetry breaking. Third-order effects, including four-wave mixing [19], two-photon absorption, saturable absorption [20–22], self action of light [23], current-induced SHG [24], and third harmonic generation [25,26], on the other hand, were shown to be remarkably strong with the $\chi^{(3)}$ estimated as high as 10^{-7} esu.

Although the SHG in crystalline graphene samples was shown to be strongly suppressed due to an in-plane inhomogeneity, this inhomogeneity can be accessed though the hyper-Rayleigh scattering (HRS) on the frequency of the optical second harmonic signal [27]. The HRS process is formed by statistically correlated fluctuation of the nonlinear-optical parameters in the plane of the sample. Assuming that the fluctuations are described by a Gaussian correlation function, which almost vanishes at the specific distance L_{Corr} (correlation length), one can obtain the following expression for the HRS scattering pattern (denoted with the 2ω superscript):

$$I^{\omega,2\omega}(\theta) \propto T^{\omega,2\omega}(\theta) \exp\left(-\left(4\pi(\sin(\theta) - \sin(\theta_0)) \frac{L_{\mathrm{Corr}}^{\omega,2\omega}}{\lambda^{\omega,2\omega}} \right)^2 \right),$$

(1)

where $T^{\omega,2\omega}(\theta)$ is the linear transmittance of the sample, θ is the angle of scattering, θ_0 is the angle between the incident wave and the reflected wave, $\lambda^{\omega,2\omega}$ are the fundamental and the SHG wavelengths. The same expression [denoted with ω superscript in Eq. (1)] can be obtained for the linear (Rayleigh) scattering from the surface of the sample with the main difference that now the fluctuations of the linear optical parameters, rather than nonlinear ones, determine the angular width and position of the scattering indicatrix. It has been shown [28,29] that a direct comparison of the linear (Rayleigh) scattering and HRS effects can give information about the structure and distribution of the scatterers beyond the capabilities of each of the methods alone. In this Letter, we report the first studies of the nonlinear scattering in multilayer graphene films.

Our specific experimental conditions are as follows. For HRS an s-polarized output of the Ti:Sapphire laser cavity at the wavelength of maximum output power around 800 nm, pulse duration 100 fs, 80 MHz repetition rate was used. The laser radiation was focused on the sample into a 50 µm spot producing about 0.8 GW/cm² peak power. The scattered SHG signal at a specific scattering angle was collected by the lens, spectrally selected with a set of Schott BG39 filters and detected by a photomultiplier tube [Fig. 2(a)]. For Rayleigh scattering, s-polarized output of a continuous wave diode laser at the wavelength 405 nm was used with no focusing on

the sample [Fig 2(b)]. Scattered light was detected by a biased photodiode. The scattering indicatrices either on the SHG wavelength of the Ti:Sapphire laser or on the wavelength of the diode laser were measured for a fixed angle of incidence of the fundamental beam as the detection system was rotated around the sample, thus, the angular dependence of the scattered light $I^{\omega, 2\omega}(\theta)$ was measured. All angles were measured relative to the incident beam.

The samples were about 10 monolayers thick, multilayer graphene films composed by CVD technique on the surface of a crystalline Ni foil, which acts as a catalyst in the process [4,14,15]. The thickness of the graphene film was controlled by the growth temperature and the gas pressure in the chamber. The metal film was subsequently removed by a wet etching process in $FeCl_3$ aqueous solution, after that the graphene film was transferred to commercially available 150 µm thick cover glass slides.

A scanning electron microscopy (SEM) image of a typical graphene film is shown in Fig. 1. Clearly resolved micrometer-sized crystal domains can be seen separated by 200–400 nm thick wrinkles at the domain boundaries. The Rayleigh scattering measured in transmission through the graphene samples shows a narrow Gaussian-shaped indicatrix centered at the transmission direction [Fig. 2(d), black squares]. Although narrow, this scattering pattern is much broader than the setup collection aperture, shown on the same figure by red circles. The linear correlation length of $L_{Corr}^{RS} \approx 1500$ nm was obtained using Eq. (1). This value can be attributed to the characteristic size of a single crystal domains in the graphene film. Similar sizes of graphene domains have been reported recently [4].

Surprisingly, HRS shows a completely different behavior with a much broader scattering pattern [Fig. 2(c)]. Nonlinear correlation length derived from the scattering indicatrix was found to be $L_{Corr}^{HRS} \approx 200$ nm. A trivial explanation of this discrepancy is a result of local surface roughness under the graphene film. The overlying graphene therefore acts a thin nonlinear screen following the morphology of the surface and producing large nonlinear scattering [29]. To rule out this mechanism, we performed the measurements of HRS in reflection (angle of incidence—60°) from 4 to 5 monolayers thick graphene samples on glass slides and oxidized silicon substrate
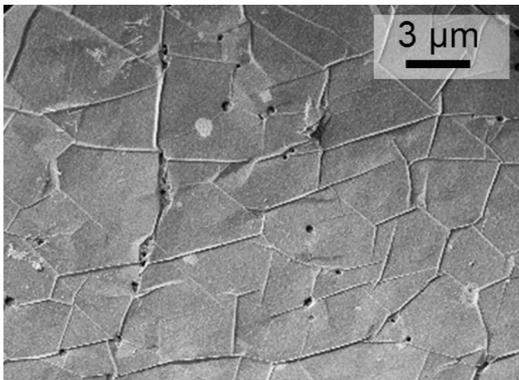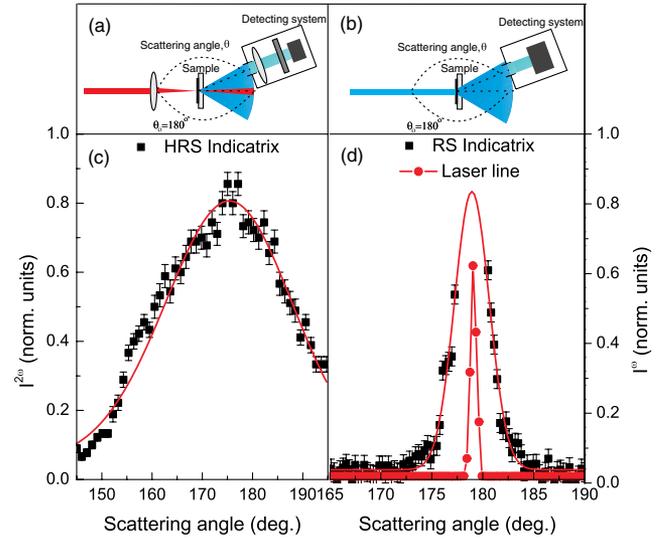

Fig. 2.   Linear and nonlinear scattering from graphene. (a) and (b) Setups for hyper-Rayleigh and Rayleigh scattering measurements, respectively, (c) HRS scattering indicatrix, and (d) Rayleigh scattering indicatrix (black squares), laser-line angular width (red circles).

(300 nm thick thermally grown oxide layer). The two corresponding HRS indicatrices are presented in the Figs. 3(a) and 3(b), respectively.

Although the estimated correlation lengths are different in value [$L_{Corr}^{HRS} \approx 250$ nm for graphene/SiO_2/Si(001) and $L_{Corr}^{HRS} \approx 450$ nm for graphene/glass], the fact they both are still far smaller than a $L_{Corr}^{RS} \approx 1.5$ µm proves that the source of the nonlinear scattering is within the graphene film and is not attributed to the substrate. Moreover, this nonlinear scattering was found to be highly robust to the parameters of the substrate as well as of the graphene film, since all the available samples, regardless of the substrate type and the thickness, reveal similar values of the correlation length that lie in the region 200–400 nm.

The only source of structural inhomogeneity of an appropriate size that is testified by our SEM microscopy images are the wrinkles that separate the crystalline domains. To prove this assumption directly, the second harmonic imaging microscopy (SHIM) was used with the 60 mW average power of a 50 fs output of the Ti:Sapphire laser cavity at 800 nm as a source. The setup of our homemade SHIM is shown in Fig. 4(a). An objective lens with a
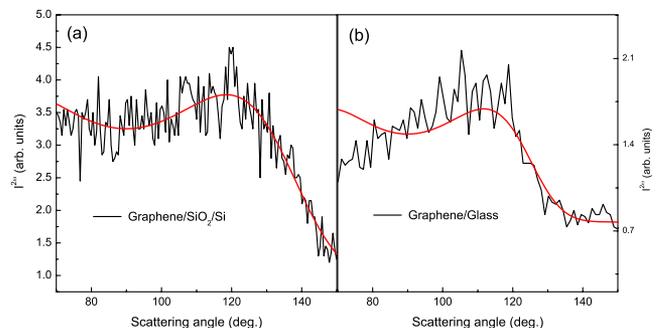

Fig. 1.   Typical SEM image of as-prepared multilayer graphene film.

Fig. 3.   HRS pattern from 4 to 5 layer thick graphene on different substrates. (a) graphene/SiO_2/Si and (b) graphene/glass. Angle of incidence—60°. Lines are theoretical fit with Eq. (1).
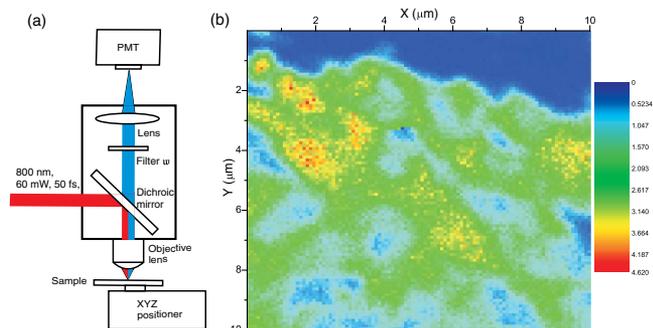
Fig. 4. (a) SHIM setup and (b) typical SHIM image from 10-layer thick graphene sample.

numerical aperture on 0.7 was used, which focused the fundamental radiation on the sample into a spot of 1.5 μm in diameter. Consequently, the spatial resolution of our SHIM setup at the second harmonic wavelength was about 700 nm.

The bare substrate without graphene coverage can be seen as a dark-blue area in the top-right corner of the image [Fig. 4(b)]. The absence of the SHG signal in this area confirms our assumptions that the second harmonic is generated mainly by graphene. The rest of the SHG image consists of wide light-blue colored areas separated by thin extended peculiarities forming a network. These peculiarities are most likely the same interdomain wrinkles that are clearly seen in the SEM image. The discrepancy between their width estimated from the SHIM (0.5–1 μm) and SEM (200–400 nm) images can be explained as a result of insufficient spacial SHIM resolution.

The question remains on the mechanism of enhanced SHG at the wrinkles between domains that are not pronounced in the linear optical scattering. It is known that single crystal graphene has 6mm symmetry, i.e., possesses a centrosymmetric structure. Thus the SHG is prohibited in the electric dipole approximation. At the same time, as was mentioned in the introduction, external influence such as mechanical stress can break this symmetry and lead to the dipole SHG. Such mechanism of the inversion symmetry breaking was already reported to be responsible for the strain-induced SHG in silicon [30] and SHG induced by the intrinsic mechanical strain in iron garnet films [31]. Other mechanisms that may lead to the enhanced SHG at the wrinkles are local field enhancement due to the curvature, variations of thickness at the boundaries reported for CVD graphene [15], or charge puddles [32] induced by local curvature of the film, and giving birth to the electric-field induced SHG [33]. Distinguishing these effects is beyond the capabilities of our current method thus further research is necessary.

To summarize, structural, optical, and nonlinear-optical studies and nonlinear-optical microscopy of multilayer graphene films deposited by CVD technique on glass and silicon substrates are performed. Two characteristic spatial scales of several microns and hundreds of nanometers are observed, which are associated with flat graphene crystal domains and with the cross section of the wrinkles that separate the domains. SHIM show that the second-order nonlinear response originates primarily from the wrinkles and is probably due to local symmetry breaking associated with mechanical stress, charge, and thickness inhomogeneities.

References

1. A. H. C. Neto, F. Guinea, N. M. R. Peres, K. S. Novoselov, and A. K. Geim, Rev. Mod. Phys. **81**, 109 (2009).
2. V. Singh, D. Joung, L. Zhai, S. Das, S. I. Khondaker, and S. Seal, Prog. Mater. Sci. **56**, 1178 (2011).
3. K. S. Novoselov, A. K. Geim, S. V. Morozov, D. Jiang, Y. Zhang, S. V. Dubonos, I. V. Grigorieva, and A. A. Firsov, Science **306**, 666 (2004).
4. K. S. Kim, Y. Zhao, H. Jang, S. Y. Lee, J. M. Kim, K. S. Kim, J.-H. Ahn, P. Kim, J.-Y. Choi, and B. H. Hong, Nature **457**, 706 (2009).
5. K. S. Novoselov, A. K. Geim, S. V. Morozov, D. Jiang, M. I. Katsnelson, I. V. Grigorieva, S. V. Dubonos, and A. A. Firsov, Nature **438**, 197 (2005).
6. R. R. Nair, P. Blake, A. Grigorenko, K. S. Novoselov, J. T. Booth, T. Stauber, N. M. R. Peres, and A. K. Geim, Science **320**, 1308 (2008).
7. A. C. Ferrari, J. C. Meyer, V. Scardaci, C. Casiraghi, M. Lazzeri, F. Mauri, S. Piscanec, D. Jiang, K. S. Novoselov, S. Roth, and A. K. Geim, Phys. Rev. Lett. **97**, 187401 (2006).
8. E. A. Obraztsova, A. V. Osadchy, E. D. Obraztsova, S. Lefrant, and I. V. Yaminsky, Phys. Status Solidi B **245**, 2055 (2008).
9. C. H. Lui, K. F. Mak, J. Shan, and T. F. Heinz, Phys. Rev. Lett. **105**, 127404 (2010).
10. L. Ju, B. Geng, J. Horng, C. Girit, M. Martin, Z. Hao, H. A. Bechtel, X. Liang, A. Zettl, Y. R. Shen, and F. Wang, Nat. Nanotechnol. **6**, 630–634 (2011).
11. J. M. B. Lopes dos Santos, N. M. R. Peres, and A. H. Castro Neto, Phys. Rev. Lett. **99**, 256802 (2007).
12. K. V. Emtsev, F. Speck, T. Seyller, L. Ley, and J. D. Riley, Phys. Rev. B **77**, 155303 (2008).
13. P. A. Obraztsov, M. G. Rybin, A. V. Tyurnina, S. V. Garnov, E. D. Obraztsova, A. N. Obraztsov, and Y. P. Svirko, Nano Lett. **11**, 1540 (2011).
14. M. G. Rybin, A. S. Pozharov, and E. D. Obraztsova, Phys. Status Solidi C **7**, 2785 (2010).
15. A. Reina, J. Xiaoting, J. Ho, D. Nezich, H. Son, V. Bulovic, M. S. Dresselhaus, and J. Kong, Nano Lett. **9**, 30 (2009).
16. M. M. Glazov, JETP Lett. **93**, 366 (2011).
17. S. Wu, L. Mao, A. M. Jones, W. Yao, C. Zhang, and X. Xu, Nano Lett. **12**, 2032 (2012).
18. J. J. Dean and H. M. van Driel, Phys. Rev. B **82**, 125411 (2010).
19. E. Hendry, P. J. Hale, J. Moger, A. K. Savchenko, and S. A. Mikhailov, Phys. Rev. Lett. **105**, 097401 (2010).
20. M. Feng, H. Zhan, and Y. Chen, Appl. Phys. Lett. **96**, 033107 (2010).
21. Q. Bao, H. Zhang, Y. Wang, Z. Ni, Y. Yan, Z. X. Shen, K. P. Loh, and D. Y. Tang, Adv. Funct. Mater. **19**, 3077 (2009).
22. V. R. Sorochenko, E. D. Obraztsova, P. S. Rusakov, and M. G. Rybin, Quantum Electron. **42**, 907 (2012).
23. H. Zhang, S. Virally, Q. Bao, L. K. Ping, S. Massar, N. Godbout, and P. Kockaert, Opt. Lett. **37**, 1856 (2012).
24. A. Y. Bykov, T. V. Murzina, M. G. Rybin, and E. D. Obraztsova, Phys. Rev. B **85**, 121413 (2012).
25. N. Kumar, J. Kumar, C. Gerstenkorn, R. Wang, H.-Y. Chiu, A. L. Smirl, and H. Zhao, Phys. Rev. B **87**, 121406 (2013).
26. S.-Y. Hong, J. I. Dadap, N. Petrone, P.-C. Yeh, J. Hone, and R. M. Osgood, Phys. Rev. X **3**, 021014 (2013).
27. K. Clays and A. Persoons, Phys. Rev. Lett. **66**, 2980 (1991).

28. A. V. Melnikov, A. A. Nikulin, and O. A. Aktsipetrov, Phys. Rev. B **67**, 134104 (2003).
29. A. A. Fedyanin, N. V. Didenko, N. E. Sherstyuk, A. A. Nikulin, and O. A. Aktsipetrov, Opt. Lett. **24**, 1260 (1999).
30. O. A. Aktsipetrov, V. O. Bessonov, T. V. Dolgova, and A. I. Maidykovskii, JETP Lett. **90**, 718 (2010).
31. P. Kumar, A. I. Maydykovskiy, M. Levy, N. V. Dubrovina, and O. A. Aktsipetrov, Opt. Express **18**, 1076 (2010).
32. M. Gibertini, A. Tomadin, F. Guinea, M. I. Katsnelson, and M. Polini, Phys. Rev. B **85**, 201405 (2012).
33. C. H. Lee, R. K. Chang, and N. Bloembergen, Phys. Rev. Lett. **18**, 167 (1967).